Ceramics International 42 (2016) 11913–11917

Contents lists available at ScienceDirect

Ceramics International

journal homepage: www.elsevier.com/locate/ceramint

Exchange-spring behavior in $BaFe_{12}O_{19}$-$Ni_{0.5}Zn_{0.5}Fe_2O_4$ nanocomposites synthesized by a combustion method

Rui Xiong *, Weiwei Li, Chunlong Fei, Yong Liu, Jing Shi

Key Laboratory of Artificial Micro- and Nano-structures of Ministry of Education and School of Physics and Technology, Wuhan University, Wuhan 430072, China

ARTICLE INFO

Article history:
Received 23 March 2016
Received in revised form
18 April 2016
Accepted 20 April 2016
Available online 23 April 2016

Keywords:
$BaFe_{12}O_{19}$-$Ni_{0.5}Zn_{0.5}Fe_2O_4$ nano-composite
Exchange spring behavior
Magnetic properties
Henkel plots

ABSTRACT

Exchange-spring systems offer various technological applications. In this study, $BaFe_{12}O_{19}$-$Ni_{0.5}Zn_{0.5}Fe_2O_4$ nanocomposite magnets with single-step hysteresis loops were synthesized through a simple combustion method. Their composition, microstructure, and magnetic properties were also investigated. It was found that the magnetic properties and the mechanisms governing the magnetization of these nanocomposite magnets are strongly influenced by the calcination temperature as well as the molar ratios of the hard and soft phases. The exchange-coupling between the hard and soft magnetic phases was confirmed by the study of Henkel plots and the variation in the magnetic properties could also be explained by the dominant role of exchange and dipolar interactions in the nanocomposites. The study provides a simple but efficient route for the fabrication of exchange-coupled nanocomposite magnets based on ferrites having controllable magnetic properties.

1. Introduction

In recent years, exchange-spring systems have gained considerable attention owing to their application in the improvement of magnetic properties [1–5]. The concept of exchange-spring behavior was put forward in the early 1990 s by Kneller et al. [6] Later, Skomski and Coey [7] proposed that the predicted magnetic energy product of ordered nanocomposites can reach up to 1 MJ/m^3 in theory, which is much larger than that of sintered Nd-Fe-B magnets (445 kJ/m^3) [8]. In the last few decades, a lot of effort has been made through theoretical as well as experimental studies to obtain materials with a high magnetic energy product. These studies mainly focused on two kinds of materials: 1) alloy composites-based permanent magnets like Nd-Fe-B, FePt, and Sm-Co [9–12] because of their high magnetic energy products and 2) oxide composite materials such as $CoFe_2O_4/Fe_3O_4$, $CoFe_2O_4/CoFe_2$, $BaCa_2Fe_{16}O_{27}/Fe_3O_4$, and $BaFe_{12}O_9/Ni_{0.8}Zn_{0.2}Fe_2O_4$ [13–16] owing to their inexpensive synthesis and high corrosion resistance. However, it is difficult to realize the exchange-spring principle in hard-soft ferrite nanocomposites because of the intricate fabrication methods and microstructural complexities involved [17]. In order to achieve homogeneously distributed hard-soft ferrite nanocomposites, a simple but efficient fabrication method is imperative.

The combustion method has gained popularity as a simple but efficient method for the fabrication of a variety of materials such as Ba-hexaferrite, NiZn ferrite, and $CoFe_2O_4$ [18–21]. Recently, some studies focusing on the fabrication of a hexaferrite/NiZn ferrite composite material using this method have been reported [22,23]. In their work, both hard and soft magnetic phases were simultaneously synthesized by the combustion method. Compared to the other methods, this “one-pot” method offers many advantages including simplicity and homogeneity. Moreover, this method can be used to fabricate exchange-spring magnets in which the average diameter of the soft phase is less than twice the domain wall width of the hard phase, which should be the case to achieve an exchange-coupling beneficial to the magnetic properties of such magnets [7]. However, these magnets usually show two-step hysteresis loops indicating that the hard and soft phases have not undergone sufficient exchange coupling at the interfaces.

In the present work, hard-soft $BaFe_{12}O_9$-$Ni_{0.5}Zn_{0.5}Fe_2O_4$ nanocomposite magnets were simultaneously fabricated by the combustion method. By controlling the fabrication conditions, homogeneously distributed hard-soft nanocomposite magnets that exhibit single-step magnetic hysteresis loops were fabricated. The nature of magnetic interactions in these composites and their magnetic properties were investigated in detail using the Henkel plot.

* Corresponding author.
E-mail address: xiongrui@whu.edu.cn (R. Xiong).

http://dx.doi.org/10.1016/j.ceramint.2016.04.114
0272-8842/

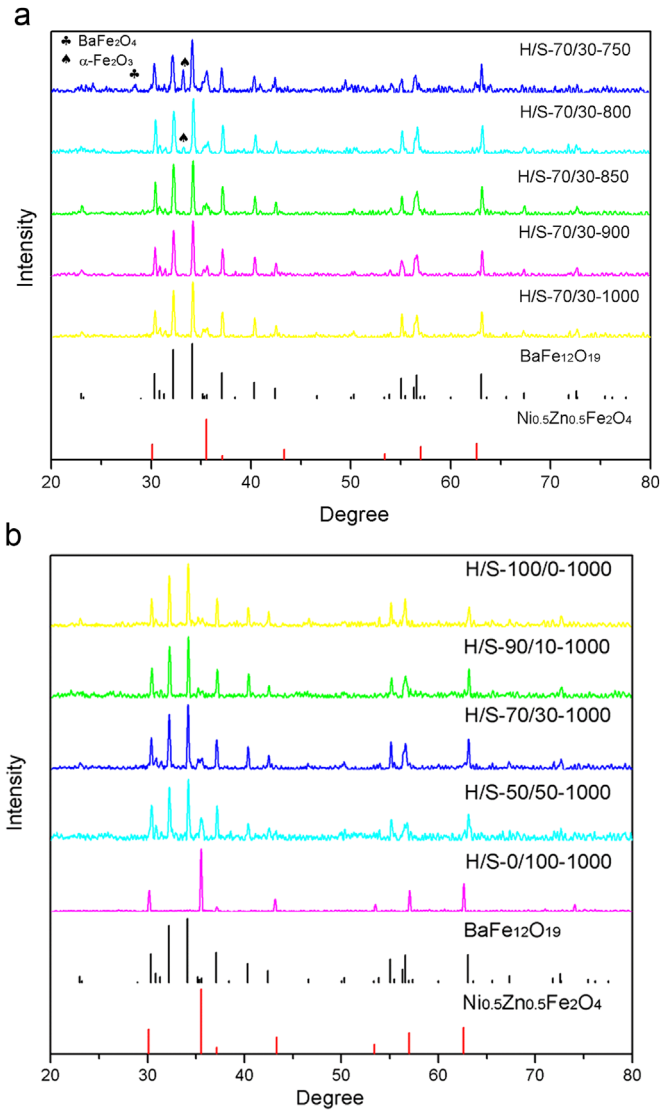

Fig. 1. a. XRD pattern of sample H/S-70/30 calcinated at different temperatures from 750 to 1000 °C. b. XRD pattern of $BaFe_{12}O_{19}$-$Ni_{0.5}Zn_{0.5}Fe_2O_4$ nano-composites with different molar ratios calcinated at 1000 °C.

2. Experiment details

The hard-soft $BaFe_{12}O_{19}$-$Ni_{0.5}Zn_{0.5}Fe_2O_4$ nanocomposite magnets were simultaneously fabricated by using the combustion method. An appropriate amount of metal nitrates and citric acid was dissolved in de-ionized water followed by the addition of ammonia solution to adjust the pH to 7. The resulting solution was then heated to 300 °C until the formation of a gel and its subsequent combustion. Finally, the resulting powders were calcined in air at 750, 800, 850, 900, or 1000 °C for 2 h in order to obtain a ferrite structure. The samples were then labeled accordingly; for example, H/S-70/30-800 denoted the sample with a hard: soft molar ratio of 70:30 calcined at 800 °C for 2 h.

XRD patterns were collected using a D8-Advanced X-ray diffractometer (XRD) with Cu kα radiation (λ=1.5418 A). The morphologies of the nanocomposites were observed by a scanning electron microscope (SEM, FEI SIRION) as well as a high resolution transmission electron microscope (HRTEM, JEM 2010 FEF). The magnetic hysteresis loops and the Henkel plots were measured at 300 K using a vibrating sample magnetometer (VSM) on a physical property measurement system (PPMS-9, Quantum Design).

3. Results and discussion

Fig. 1(a) shows the XRD patterns of the H/S-70/30 nanocomposites calcined at different temperatures. The XRD patterns of the samples calcined at 750 °C and 800 °C show the presence of $BaFe_2O_4$ and α-Fe_2O_3 impurity phases. At higher calcination temperatures, only $BaFe_{12}O_{19}$ and $Ni_{0.5}Zn_{0.5}Fe_2O_4$ phases are observed and no impurity phase is detected.

The XRD patterns of the $BaFe_{12}O_{19}$-$Ni_{0.5}Zn_{0.5}Fe_2O_4$ nanocomposites with different molar ratios calcined at 1000 °C are shown in Fig. 1(b). As can be seen, the characteristic peaks for both the hard ($BaFe_{12}O_{19}$) and soft ($Ni_{0.5}Zn_{0.5}Fe_2O_4$) phases are observed and no extra peak is detected within the resolution of the diffractometer.

Fig. 2 shows the SEM, TEM, and HRTEM images of the H/S-70-30-1000 nanocomposite. The average diameter of the particles was estimated to be about 100 nm. The HRTEM images confirm the presence of the hard and soft magnetic phases and indicate their boundaries. The insets in Fig. 2 provide details of the interplanar distance in both the phases. The lattice fringes matched well with the theoretical reflections for $BaFe_{12}O_{19}$ (P6/mmm symmetry) and $Ni_{0.5}Zn_{0.5}Fe_2O_4$ (Fd 3m atomic model).

Fig. 3(a) shows the magnetic hysteresis loops of the H/S-70/30 nanocomposites calcined at different temperatures. It can be observed that there exists a two-step hysteresis loop for the powder calcined at 750 °C. The powder calcined at 800 °C shows a much smoother hysteresis loop. The powders calcined at temperatures higher than 800 °C show single-step hysteresis loops, indicating the occurrence of strong exchange-coupling at the interfaces between the hard and soft magnetic phases. If the exchange-coupling is not strong enough, the resulting hysteresis loop would be the superimposition of two loops corresponding to the soft and hard phases [14].

Saturation magnetization (*Ms*) was obtained by fitting the initial magnetization curve (above 45,000 Oe) using the Law of Approach to Saturation [24].

$$M = Ms - \frac{0.07619K_{eff}^2}{MsH^2} + \chi_p H \quad (1)$$

where *M* and *H* denote the magnetization and applied magnetic field, respectively, and *A* is a parameter which is related to the effective magnetic anisotropy constant. The final term represents the magnetization contributed by the paramagnetic magnetization process at a high field. Remanence (*Mr*) and coercivity (*Hc*) were determined by linear fitting the data near *H*=0 Oe and *M*=0 emu/g, respectively.

The magnetic properties of the nanocomposites calcined at different temperatures are shown in Fig. 3(b). As can be seen, *Ms* as well as *Mr* increased with an increase in the calcination temperature. *Hc* shows a maximum value at 800 °C, which starts decreasing as the calcination temperature is increased further. It is well-known that an increase in calcination temperature leads to an increase in average particle size. This might have contributed to the increase in *Ms* and *Mr*. According to micromagnetic calculations, the size of soft grains should ideally not be larger than twice the domain wall width of the hard magnetic phase [7]. The increase in grain size increases the dipolar interactions among the soft phases and enervates the exchange force between the hard and the soft phases. As a result, the reverse domains in the soft phases with low nucleation field can be nucleated easily, thus decreasing the coercivity.

The magnetic hysteresis loops for the samples calcined at 1000 °C with different molar ratios are shown in Fig. 4. It is observed that all the samples show single-step hysteresis loops. The magnetic properties are listed in Table 1. The magnetic property of